

## 39.2: Optical Analysis of Vertical Aligned Mode on Color Filter Liquid-Crystal-on-Silicon Microdisplay

B. L. Zhang, H. S. Kwok, and H. C. Huang

Centre for Display Research, Hong Kong University of Science and Technology, Clear Water Bay, Hong Kong

Y. C. Chen

Himax Display, No.12, Nanke 8<sup>th</sup> Road, Tainan Science-based Industrial Park, Tainan, Taiwan

### Abstract

We report our studies of vertical aligned mode on color filter liquid-crystal-on-silicon microdisplay. Three-dimensional optical analyses were performed to minimize fringing field effect in small color pixels. The simulation results were compared with experimental data and also the results of twisted nematic mode.

### 1. Introduction

We have developed a color filter liquid-crystal-on-silicon (CF-LCOS) microdisplay that integrated color filters on silicon. In our previous works, we have presented process, characterization and optical modeling of this breed of CF-LCOS microdisplays in twisted nematic (TN) mode [1, 2]. We used either rubbed or photo-aligned method [3] for these microdisplays, and they worked well for near-to-eye or mini-projector which had light illumination below 8 million lux. However, the display performance started to degrade when the light illumination exceed 15 million lux. The color filter can still resist strong light illumination. But the rubbed or photo-aligned layer was suffered from strong light illumination, especially the ultra-violet part of the light, and the contrast and color saturation of the display was accordingly degraded.

In this paper, we report our studies of vertical aligned (VA) mode on the CF-LCOS microdisplays. The use of inorganic silicon oxide as the alignment layer could improve light stability of the microdisplays. We therefore applied this technology to CF-LCOS microdisplays, and at the same time, configured the microdisplays to VA mode for better contrast [4]. Three-dimensional optical analyses were performed to analyse and optimize these VA CF-LCOS microdisplays, and also provided guidelines for experiments.

### 2. Process of VA CF-LCOS Microdisplays

The assembly process of the VA mode is very similar to that of the conventionally TN mode, except the alignment layer. Though there are special polyimide layers that can be spun and coated on the silicon or glass substrate as the alignment layer for the VA mode [5, 6]. Their pretilt angles were limited and they had light stability problem due to the polyimide base alignment layer. Therefore, at present, the majority of the LCOS microdisplays of VA mode used the silicon oxide as the alignment layer [7-11].

In the process of the CF-LCOS microdisplay of the VA mode, the silicon oxide was also adopted as the alignment layer. The color filter silicon substrate was prepared by the same process as reported in our previous works [1]. The color filter array was again 0.75 $\mu\text{m}$  for all three colors. Then, a thin layer of silicon oxide was sputtered on the silicon substrate as the alignment layer. Thereafter, a CF-LCOS microdisplay of VA mode was assembled with a cell gap of 3 $\mu\text{m}$ . And a LC mixture, MLC-6608

( $n_e=1.5578$ ,  $n_o=1.4748$  and  $\Delta\epsilon=-4.2$ ) from Merck, was used for the assembly of the microdisplay.

The pretilt angle of the silicon oxide alignment layer on the glass plate was 85°. However, it was very difficult to measure the pretilt angle on the silicon substrate with the color filter array. It was also found that the uniformity of the pretilt angle was poor from the appearance of the microdisplay. It was believed that the silicon oxide layer on top of the color filter array was greatly dispersed and could not maintain uniform pretilt angle. As a result, the VA mode could not be kept up and the microdisplay lost its display function. It was further believed that an improvement of the flatness of the color filter array and increase of the thickness of the silicon oxide layer could improve the stability of the VA mode on the CF-LCOS microdisplays. But it was beyond the scope of this paper. In this paper, emphasis would be placed on the optical modeling and optimization of the CF-LCOS microdisplay of the VA mode.

### 3. Optical Modeling

The optical modeling of the VA mode was more or less the same as that of the TN mode as reported in our previous works [2]. Fig. 1(a) showed the top view of the simulation structure. There were two pixels in the simulation structure and each pixel included three sub-pixels of red, green and blue. The sub-pixels were arranged in delta shape and had a pitch of 10 $\mu\text{m}$  by 7.5 $\mu\text{m}$  with a pixel gap of 0.5 $\mu\text{m}$ . Cross section of the simulation structure was also shown in Fig. 1(b). In this arrangement, the LC cell was driven in frame inversion in which the green sub-pixel was 0V and the red and blue sub-pixels were 4V. The color filter array was 0.75 $\mu\text{m}$  thick and the LC cell gap was 3 $\mu\text{m}$  in the simulation.

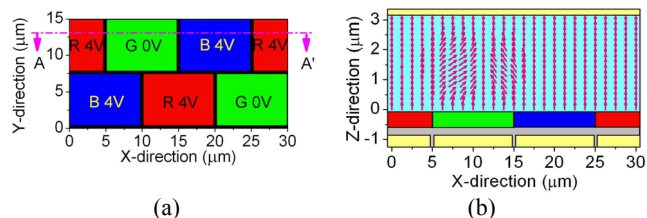


Fig. 1 (a) Top and (b) cross section of the simulation structure.

The common voltage on the top electrode was kept at a constant voltage of 5V. As a result, the sub-pixel of 0 and 4V produced a root-mean-squared voltage of 5 and 1V, respectively, across the color filter and LC layers. For a fair comparison with the experimental data, the same LC mixture, MLC-6608 from Merck, was used for the simulation.

The simulated director distribution of the VA mode on the CF-LCOS structure was also shown in Fig. 1(b). With the homeotropic alignment, the LC molecules were aligned perpendicular to the surface of the substrate in off-state as shown

by the red and blue sub-pixels in Fig. 1(b). At this state, the LC layer introduced zero birefringence to the incident polarized light, and hence a perfect dark state was resulted through cross polarizers. This good dark state could ensure high contrast of the display. The LC mixtures used in the VA mode had a negative dielectric anisotropy. When an electric field was applied, the LC molecules were lined up and parallel to the surface of the substrate as shown by the green sub-pixel in Fig. 1(b).

The simulated spatial optical reflectance of the VA CF-LCOS microdisplay with 88° pretilt angle was shown in Fig. 2. In this image, the green sub-pixels were turned. But they were observed with dark disclination lines and divided into four domains with a shape of windmill. The simulated color coordinate of this green image with a LED light source was (0.237, 0.610), which was very good due to very dark red and blue sub-pixels. In comparison, the color coordinates were only (0.247, 0.585) for the MTN mode [2].

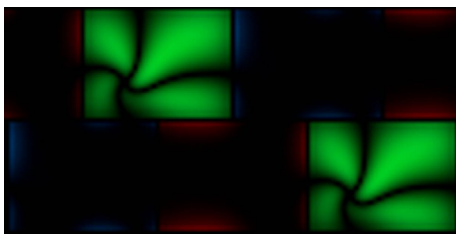


Fig.2 The simulated spatial optical reflectance of the VA CF-LCOS microdisplay.

But the brightness of the green image was obviously reduced since the ON region of the bright area did not occupy the whole green sub-pixels. Fig. 3 shows the simulated reflectivity of the color images for both the color MTN and VA CF-LCOS microdisplays. The simulated peak reflectivity of the green image was only 4.7%, which was much smaller than 13% of the MTN mode. The simulated optical reflectance of red and blue images had similar low values. This low optical reflectivity of color images should be improved in order to apply the VA mode to the CF-LCOS microdisplays.

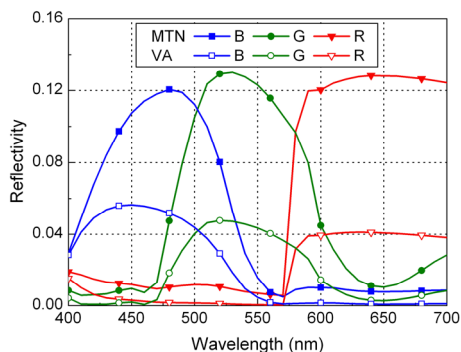


Fig. 3 The simulated reflectivity of the color images for both the MTN and VA CF-LCOS microdisplays.

With an attempt to verify the accuracy of this 3D optical modeling of the VA mode, the simulated spatial optical reflectance was compared with the observed optical reflectance of the CF-LCOS microdisplay sample introduced in Section 2. Fig. 4(a) showed the observed spatial optical reflectance of the VA CF-LCOS microdisplays. It should be noted that the sputtered oxide should produce an 85° pretilt angle on the color filter substrate, but this pretilt angle was difficult to be measured and confirmed. It was

believed that the pretilt angle should be smaller than 85° due to the topography of the color filter array. With the systematic comparisons, we found that the simulation result of 80° pretilt angle, which was shown in Fig. 4(b), coincided with the experimental one very well.

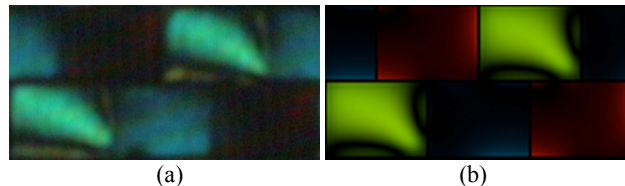


Fig. 4 (a) Observed and (b) simulated spatial optical reflectance of the CF-LCOS microdisplays of VA mode.

## 4. Optimizations

With this 3D optical analysis as a tool, we were able to locate the disclination lines and minimize the color fringing field accordingly. In this section, the color purity and reflectivity of the pixel array were compared with respect to pretilt angle and pixel size. A circularly polarized optical arrangement was proposed to minimize the fringing field of the VA mode.

### 4.1 Pretilt Angle

Pretilt angle is an important parameter to determine the performance of the VA CF-LCOS microdisplays. Contrast ratio, response time, color purity and optical reflectance are all related to the pretilt angle [12-14]. Fig. 5 showed the simulated spatial optical reflectance of the color pixel array with pretilt angle reduced from 90° to 80°. There were four symmetrical LC domains when the pretilt angle was 90°. At this angle, there was no preferable rotational direction for LC molecules when a voltage was applied. As a result, each quadrant has a symmetrical pattern, which was denoted as d1, d2, d3 and d4 as also shown in Fig. 5(a) for easier referring and descriptions later.

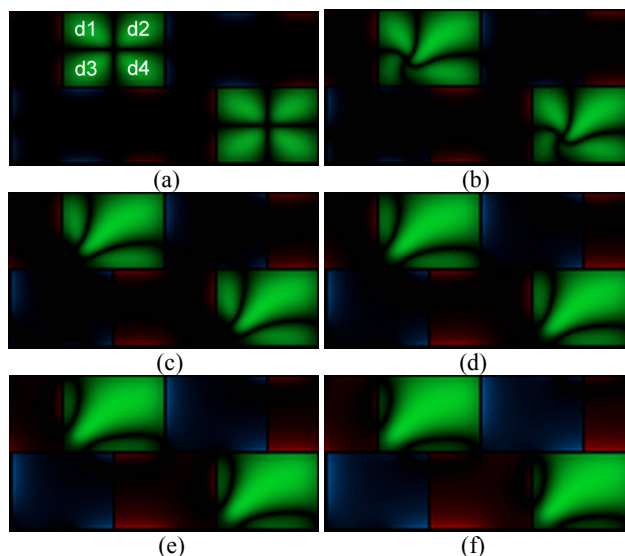


Fig. 5 The evolution of simulated spatial optical reflectance of color pixel array with pretilt angle of (a) 90°, (b) 88°, (c) 86°, (d) 84°, (e) 82°, and (f) 80°.

When the pretilt angle was reduced from 90° toward 80°, the center of declination lines had the tendency to be moved toward

the bottom-left corner of the ON pixel. As a result, domain d1, d3 and d4 were shrunk to a smaller size. On the contrary, domain d2 was enlarged. When the pretilt angle was reduced to  $86^\circ$ , domain d2 and d3 were combined and three domains were resulted in the ON pixels. As the pretilt angle was further reduced, the combined d2 and d3 domain was further increased and occupied more area of the ON pixel. Obviously, the optical reflectance of the ON pixels was increased. However, the dark state in the off-pixels was degraded due to the residue birefringence, which was caused by smaller pretilt angle. This resulted in the light leakage in dark red and blue sub-pixels and degraded the color and contrast of device at  $80^\circ$  pre-tilt angle, which is clearly shown Fig. 5(f).

Fig. 6 showed the peak reflectivity and contrast of the VA CF-LCOS microdisplays with respect to pretilt angle. The peak reflectivity of green image was increased from 4.52 to 8.43% when the pretilt angle was reduced from  $90^\circ$  to  $80^\circ$ . Similarly, the peak reflectivity of red and blue images was increased from 3.79 to 7.86% and 5.49 to 8.62%, respectively. On the other hand, the contrast was dropped rapidly from infinity at the pretilt angle of  $90^\circ$  to  $10^2$  at the pretilt angle of  $80^\circ$ . We believed that  $86^\circ$  was the optimal pretilt angle for the VA CF-LCOS microdisplays. At this angle, the peak reflectivity of green image was 5.7% and the contrast was in the order of  $10^4$ .

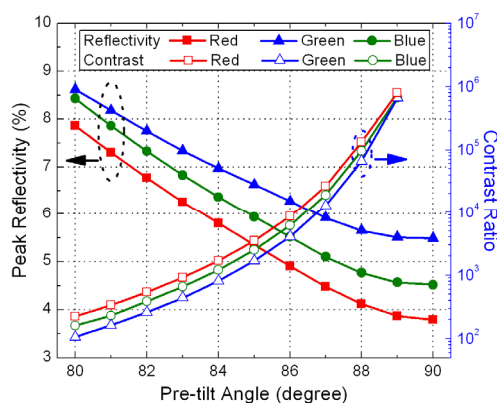


Fig. 6 The peak reflectivity and contrast of the VA CF-LCOS microdisplays with respect to pretilt angle.

## 4.2 Pixel Size

The relation of optical reflectance and color purity with respect to pixel size could also be studied with this 3D optical modeling. The spatial optical reflectance of the color pixel arrays were simulated, which had a pixel pitch of 12, 15, 18, and  $21\mu\text{m}$ , respectively. The pretilt angle was  $86^\circ$  and the cell gap was  $3\mu\text{m}$  in the simulation.

All these pixels had a similar pattern or LC domains as shown in Fig. 5(c), since the pretilt angle was the same. However, the percentage of the bright image in the ON pixel was increased with larger pixel size. As a result, the color purity was also increased with respect to the pixel size. It was found that the color coordinates of green image were improved from (0.237, 0.607) at  $12\mu\text{m}$  to (0.237, 0.610) at  $15\mu\text{m}$ , to (0.237, 0.613) at  $18\mu\text{m}$  and to (0.238, 0.615) at  $21\mu\text{m}$  pixel. Similarly, the red and blue color purity was also increased slightly from (0.628, 0.300) and (0.134, 0.169) at  $12\mu\text{m}$ , to (0.636, 0.301) and (0.133, 0.170) at  $15\mu\text{m}$ , to (0.644, 0.302) and (0.133, 0.170) at  $18\mu\text{m}$ , and to (0.650, 0.303) and (0.132, 0.171) at  $21\mu\text{m}$  pixel, respectively.

The peak reflectivity of color images was also increased with pixel size. It was found that the peak reflectivity of green image was increased from 4.45% of the  $12\mu\text{m}$  to 5.52% of the  $15\mu\text{m}$ , to 6.37% of the  $18\mu\text{m}$  and to 7.08% of the  $21\mu\text{m}$  pixel. Similarly, the overall optical reflectance of red and blue is also increased from 3.86% and 5.18% of the  $12\mu\text{m}$  to 4.91% and 6.28% of the  $15\mu\text{m}$ , and to 5.80% and 7.11% of the  $18\mu\text{m}$ , and to 6.56% and 7.78% of the  $21\mu\text{m}$  pixel, respectively. It should be noted that the overall brightness of the pixel array were the same since there was no fringing field when all the red, green, and blue pixels were turned on and off at the same voltage. The increase of the pixel size would increase the color saturation and brightness of individual color.

## 4.3 Circularly Polarized Vertical Alignment

In addition to the linearly polarized optical arrangement of the VA cell, circularly polarized VA (CP-VA) cells have recently been studied for better contrast and reflectance. For example, Y. Iwamoto and his co-workers have studied the use of fringing electrical field to produce multi-domain VA LCD by circular polarizer and named this new display as FEF-MVA-LCD [15, 16]. As the input light was circularly polarized, the disclination lines in the ON pixel could be eliminated and the optical efficiency or brightness of this display would be greatly improved. Fan Chiang and his co-workers applied a similar circularly polarized optical arrangement to the monochrome LCOS microdisplay and studied its optical properties with a 2D optical analysis [17]. This microdisplay, referred as CP-VA LCOS microdisplay, had improved optical efficiency compared with the conventional one.

In this paper, the 3D optical modeling was also applied to study the VA CF-LCOS microdisplays with circular polarizers. The simulation structure was the same as that was described in section 2, but circular polarizers were used instead of cross linear polarizers. The circular polarizer was modeled as a linear polarizer laminated with a quarter wave plate whose optical axis is oriented at  $45^\circ$  to the x-axis. Fig. 7 showed the simulated spatial optical reflectance of the VA CF-LCOS microdisplay with circular and linear polarizers. For the ease of description, the VA CF-LCOS microdisplay with circular polarizers and linear polarizers were referred as CP-VA and LP-VA CF-LCOS microdisplay in this paper, respectively.

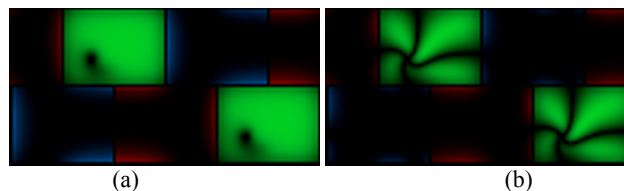


Fig. 7 The simulated spatial optical reflectance of (a) CP-VA and (b) LP-VA CF-LCOS microdisplays.

The dark area observed in the LP-VA CF-LCOS microdisplay as shown in Fig. 7(b) was due to the azimuthal orientation of LC directors around the dark disclination lines, which coincided with the transmission axes of the linear polarizers [15, 16]. With circular polarizers, the majority of the dark disclination lines were removed. However, there was still a dark spot, which could be observed in the center position of the disclination lines, as shown in Fig. 7(a).

To illustrate the generation of this dark spot, the LC director distribution in the middle plane of the LC cell was simulated and

shown in Fig. 8. When a voltage was applied, the LC directors were rotated parallel to the middle plane except the center of the dark spot. Although the LC directors outside this dark spot were arranged in centrifugal directions, they were all parallel to the azimuthal direction of the plane. And the optical reflectance through circular polarizers was bright. In the dark spot, the LC directors were pushed and squeezed to the vertical direction due to the counter-centrifugal forces from the perimeter parallel LC directors. As a result, the optical reflectance through the circular polarizers was dark.

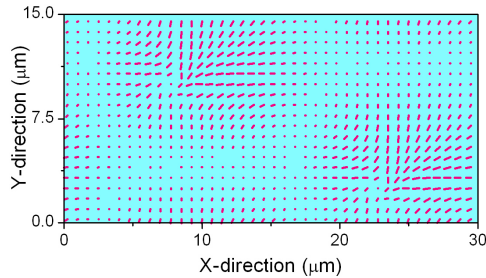


Fig. 8 The LC director distribution in the middle plane of the LC cell.

With more bright area in the ON pixel of the CP-VA CF-LCOS microdisplay, the optical reflectance of color images were greatly improved. The simulated optical reflectance of green image in the CP-VA CF-LCOS microdisplay was 11.4%, which was the double of that in the LP-VA CF-LCOS microdisplay. At the mean time, there was no color leakage in OFF pixel since all the LC molecules were still vertically positioned. As a result, the contrast and color saturation were still maintained at good values. The simulated color coordinate of the green image in the CP-VA CF-LCOS microdisplay was (0.237, 0.594), which was comparable with (0.237, 0.610) in the LP-VA CF-LCOS microdisplay.

Although the CP-VA CF-LCOS microdisplay had higher optical reflectance, it could not be applied to the single-panel projector architecture with one PBS, which was natural for crossed linear polarizers. To modify the single-panel projector architecture for CP-VA LCOS microdisplay, the PBS should be replaced by a BS for simple beam splitting without linear polarization. Thereafter, circular polarizers would be placed before and after the light coming into and going out of the BS as pre- and post-polarizers, respectively. In this arrangement, half of the light did not go through the BS to the panel, and the overall system efficiency was reduced by a half. The CP-VA CF-LCOS microdisplay had the merit of bright color images, but the corresponding optical architecture for projectors has to come out to utilize this advantage.

## 5. Conclusions

We present a 3D optical analysis of fringing effect in small color pixels on VA CF-LCOS microdisplays. Experiments were performed to evaluate the simulation accuracy, and the simulated optical reflectance agreed well with the experimental ones. With this 3D optical analysis as a tool, we analyzed and optimized color pixels with respect to pretilt angle, pixel size and optical

polarization. The dependence of the disclination lines with respect to pretilt angle and fringing field effect was discussed. With optimal pretilt angle and pixel size, the optical efficiency would be increased without sacrificing much contrast and color saturation. It was also found that the CP-VA mode could improve greatly the optical efficiency, but a corresponding projector structure has to come out to utilize this advantage.

## 6. Acknowledgements

This work is partially supported by the Research Grant Council of the Government of the Hong Kong Special Administrative Region.

## 7. References

- [1] H. C. Huang, B. L. Zhang, H. S. Kwok, P. W. Cheng, and Y. C. Chen, *Soc. for Info. Disp. Symp. Digest*, 880 (2005).
- [2] B. L. Zhang, H. S. Kwok, and H. C. Huang, *J. of Appl. Phys.*, **98**, 123103 (2005).
- [3] B. L. Zhang, K. K. Li, V. G. Chigrinov, H. S. Kwok, and H. C. Huang, *Jpn. J. Appl. Phys.*, **44**, 3983 (2005).
- [4] S. Shimizu, Y. Ochi, A. Nakano, and M. Bone, *Soc. for Info. Disp. Symp. Digest*, 72 (2004).
- [5] J. Kim, S. Kim, K. Park, and T. Kim, *Soc. for Info. Disp. Symp. Digest*, 806 (2001).
- [6] V. Kononov, V. Chigrinov, H. S. Kwok, H. Takada, and H. Takatsu, *Jap. J. of Appl. Phys.*, **43**, 261 (2004).
- [7] *Microdisplay Report*, **6**, 1 (2003).
- [8] R. D. Sterling and W. P. Bleha, *Int. Disp. Works.*, 809 (1997).
- [9] A. Nakano, A. Honma, S. Nakagaki, and K. Doi, *Int. Soc. Opt. Eng. Proceedings of SPIE*, **3296**, 100 (1998).
- [10] T. Katayama, H. Natsuhori, T. Moroboshi, M. Yoshimura, and M. Hayakawa, *Soc. for Info. Disp. Symp. Digest*, 976 (2001).
- [11] S. Shimizu, Y. Ochi, A. Nakano, and M. Bone, *Soc. for Info. Disp. Symp. Digest*, 72 (2004).
- [12] H. D. Smet, D. Cuypers, A. V. Calster, J. V. D. Steen, and G. V. Doorslaer, *Displays*, **23**, 89 (2002).
- [13] A. V. Calster and D. Cuypers, *Proceedings of SPIE*, **3954**, 112 (2000).
- [14] D. Cuypers, H. D. Smet, and A. V. Calster, *Soc. for Info. Disp. Symp. Digest*, 1298 (2005).
- [15] Y. Iwamoto and Y. Iimura, *Jpn. J. Appl. Phys.* **41**, L1383 (2002).
- [16] Y. Iwamoto and Y. Iimura, *Jpn. J. Appl. Phys.* **42**, L51 (2003).
- [17] K. H. Fan Chiang, X. Y. Zhu, S. T. Wu, and S. H. Chen, *Soc. for Info. Disp. Symp. Digest*, 1290 (2005).